The Role of Nonlinear Substrate Elasticity in the Wrinkling of Thin Films

Share Your Story

The Harvard community has made this article openly available.
Please share how this access benefits you. Submit a story .

Accessibility

The role of nonlinear substrate elasticity in the wrinkling of thin films*

John W. Hutchinson**

School of Engineering and Applied Sciences

Harvard University, Cambridge, MA 01238 USA

Abstract The role of substrate nonlinearity on the stability of wrinkling of thin films bonded to compliant substrates is investigated within the initial post-bifurcation range when wrinkling first emerges. A fully nonlinear neo-Hookean bilayer composed of a thin film on a deep substrate is analyzed for a wide range of the film/substrate stiffness ratio, from films that are very stiff compared to the substrate to those only slightly stiffer. Substrate pre-stretch prior to film attachment is shown to have a significant effect on the nonlinearity relevant to wrinkling. Two dimensionless parameters are identified which control the stability and mode shape evolution of the bilayer: one specifying arbitrary uniform substrate pre-stretch and the other a stretch-modified modulus ratio. For systems with film stiffness greater than about five times that of the substrate the wrinkling bifurcation is stable, while for systems with smaller relative film stiffness bifurcation can be unstable, especially if substrate pre-stretch is not tensile.

Key words: winkling, wrinkling stability, thin films, neo-Hookean elasticity

1. Introduction

For many film-substrate systems, compressive buckling of the film into a wrinkling mode is a phenomenon to be avoided. This view motivated much of the early work on wrinkling such as that of Allen (1969) on structural composite panels having stiff outer skins and thick compliant cores. In recent years, new motivation for studying wrinkling has arisen wherein the

phenomenon has become a desirable means to generate micron-to-millimeter scale surface patterns for a wide range of applications involving soft materials. The emphasis in studying wrinkling has shifted to understanding the patterns that emerge and how they can be selected and manipulated. Applications include textured surfaces for biological applications, for altering wettability, adhesion and haptic characteristics, for flexible electronics, and for controlling fluid flow within boundary layers. Overviews of recent developments related to wrinkling and some of its applications are available in Genzer & Groenewold (2006) and Li et al. (2012).

Much of the recent thrust on wrinkling takes place within the context of research on soft elastomeric substrate materials characterized by low stiffness and substantial elasticity. Moreover, the range of stiffness of the materials being employed, as measured by elastic modulus, is extraordinary, greatly expanding the parameter space of for wrinkle pattern design. Film/substrate systems with metal or ceramic films deposited on polymers or elastomers can have a film/substrate modulus ratio as large as ten thousand. Systems formed by oxidizing the surface of a material such as polydimethylsiloxane (PDMS) have silica-like films with modulus ratios in the range from one to ten thousand (Chan & Crosby, 2006). Systems having polymer films bonded to elastomer substrates will have lower modulus ratios. For example, lower modulus ratios have been produced and studied by Yin, et al. (2012) with films chemically deposited on PDMS: a ratio of 4 for hydroxyethl methacrylate films and 17 for ethylene glycol diacrylate films. Biological systems often have skins with a modulus only slightly above that of the underlying substrate (Genzer & Groenewold, 2006; Yin, et al., 2008).

The above observations motivate one aspect of the present study: the investigation of wrinkling over a range of film/substrate stiffness ratio from only slightly greater than unity to very large. This aspect builds on earlier studies by Cai and Fu (1999) and Cao and Hutchinson (2012a) where bifurcation of a neo-Hookean bilayer was studied over the full range of modulus ratios. Here, the emphasis is on the stability of the wrinkling bifurcation and the evolution of the wrinkle mode shape as the system is compressed beyond the critical bifurcation strain. Under plane strain compression, models based on a linear substrate response predict stable wrinkling behavior with no evolution in mode shape. Substrate nonlinearity underlies the main concerns of interest in this paper. The paper begins by presenting some generally applicable analytical results on the nonlinear response of a pre-stretched neo-Hookean half-space subject to sinusoidal

surface loadings. As further background, a brief summary is presented in Section 3 of the classical results on plane strain wrinkling behavior based on the widely adopted model for stiff films attached to compliant linear substrates. Section 4 presents the results of the initial post-bifurcation analysis of the neo-Hookean bilayer, with calculation details provided in the Appendix. The analysis accounts for the possibility of a general uniform pre-stretch imposed on the substrate prior to film attachment. The release of tensile substrate pre-stretch is commonly used as a technique to generate film compression. It will be seen that substrate pre-stretch can have a significant effect on wrinkling behavior, due to its effect on nonlinearity, and is thus another potential means of manipulating wrinkling patterns.

2. Nonlinear response of a neo-Hookean substrate to sinusoidal loadings

In this section the results of a perturbation analysis are presented characterizing the nonlinear response of a semi-infinite neo-Hookean substrate subject to a combination of uniform pre-stretch and periodic surface tractions. The central results, which will be used to interpret thin film wrinkling, are presented in this section, with details of the analysis given in the Appendix. The geometry and notation is shown in Fig. 1. Lagrangian coordinates, (x_1, x_2, x_3), associated with locations of material points in the undeformed state are used throughout this paper with vector and tensor components defined relative to the corresponding Cartesian base vectors. The surface of the undeformed half-space coincides with the plane $x_2 = 0$ with the substrate lying below. A uniform pre-stretch characterized by $(\lambda_1, \lambda_2, \lambda_3)$ with $\lambda_1 \lambda_2 \lambda_3 = 1$ is imposed on the substrate with displacements $u_i = (\lambda_i - 1)x_i$ (no sum on i) such that the surface remains coincident with the plane $x_2 = 0$. In addition to the pre-stretch, the loading produces plane strain deformations of the substrate that are periodic with period ℓ with respect to x_1 and decay to zero as $x_2 \to -\infty$. The total displacements are

$$u_1 = (\lambda_1 - 1)x_1 + U_1(x_1, x_2), \quad u_2 = (\lambda_2 - 1)x_2 + U_2(x_1, x_2), \quad u_3 = (\lambda_3 - 1)x_3 \tag{1}$$

Throughout this paper, λ_3 is taken as fixed and λ_1 is regarded as the prescribed stretch such that the ratio $r = \lambda_2 / \lambda_1 = 1 / \lambda_1^2 \lambda_3$ is determined by λ_1.

The neo-Hookean substrate material is incompressible with ground state shear modulus μ_S. Nominal tractions acting on the substrate surface (force per undeformed area) are denoted by $T_\alpha(x_1)$ ($\alpha = 1, 2$) and these have zero average and period ℓ with respect to the coordinate x_1. The change in energy of the loaded substrate (per unit distance x_3 and per wavelength ℓ) from that in the uniformly pre-stretched state is (Cao and Hutchinson, 2012b):

$$\Phi(\lambda_i, \mathbf{U}, Q) = \mu_S \int_0^\ell \int_{-\infty}^0 I(\lambda_i, \mathbf{U}, Q) dx_2 dx_1 - \int_0^\ell T_\alpha U_\alpha dx_1 \tag{2}$$

with

$$I(\lambda_i, \mathbf{U}, Q) = \frac{1}{2}\left(U_{1,1}{}^2 + U_{2,2}{}^2 + U_{1,2}{}^2 + U_{2,1}{}^2\right) - Q\left(\lambda_2 U_{1,1} + \lambda_1 U_{2,2}\right) \\ - (r + Q)\left(U_{1,1} U_{2,2} - U_{1,2} U_{2,1}\right) \tag{3}$$

In (2), the tractions are regarded as prescribed and Q is a Lagrangian multiplier introduced to enforce the incompressibility condition:

$$\lambda_2 U_{1,1} + \lambda_1 U_{2,2} + U_{1,1} U_{2,2} - U_{1,2} U_{2,1} = 0 \tag{4}$$

The Euler equations obtained by rendering Φ stationary with respect to ($\mathbf{U}, Q$) are (4) and

$$\nabla^2 U_1 - \lambda_2 Q_{,1} - Q_{,1} U_{2,2} + Q_{,2} U_{2,1} = 0 \tag{5}$$

$$\nabla^2 U_2 - \lambda_1 Q_{,2} - Q_{,2} U_{1,1} + Q_{,1} U_{1,2} = 0 \tag{6}$$

The surface tractions are given by

$$T_1 = \mu_S \left(U_{1,2} + (r + Q)U_{2,1}\right)_{x_2=0}, \quad T_2 = \mu_S \left(U_{2,2} - (r + Q)U_{1,1} - \lambda_1 Q\right)_{x_2=0} \tag{7}$$

The form of the equations based on coordinates defined with respect to the undeformed state will be used to produce the solutions in this paper. Nevertheless, the following change of variables reveals that the solution to the traction boundary value problem depends on the single pre-stretch parameter, $r = \lambda_2 / \lambda_1 = 1 / \lambda_1{}^2 \lambda_3$, together with a stretch modified shear modulus,

4

μ_S / λ_3 . Specifically, define coordinates with respect to material points in the uniform pre-stretched state by $\overline{x}_i = \lambda_i x_i$ (no sum). The energy change defined in (2) is

$$\Phi(\lambda_i, \mathbf{U}, Q) = \lambda_3 \left\{ \mu_S \lambda_3^{-1} \int_0^{\overline{\ell}} \int_{-\infty}^0 \overline{I}(r, \mathbf{U}, Q) r^{-1} d\overline{x}_1 d\overline{x}_2 \; - \int_0^{\overline{\ell}} \overline{T}_\alpha U_\alpha d\overline{x}_1 \right\}$$

where $\overline{\ell} = \lambda_1 \ell$, $\overline{T}_\alpha = T_\alpha / \lambda_1 \lambda_3$ is the nominal traction per pre-stretched area, and

$$\overline{I}(r, \mathbf{U}, Q) = \frac{1}{2} \left(U_{1;1}{}^2 + r^2 U_{2;2}{}^2 + r^2 U_{1;2}{}^2 + U_{2;1}{}^2 \right) - Qr \left(U_{1;1} + U_{2;2} \right)$$
$$- r(r+Q) \left(U_{1;1} U_{2;2} - U_{1;2} U_{2;1} \right)$$

with $( )_{;j} = \partial( ) / \partial \overline{x}_j$. Thus, any $\left(U_\alpha, Q, \overline{T}_\alpha \right)$ rendering Φ stationary will depend only on r and μ_S / λ_3 . At various points in this paper, it will be useful to switch between variables defined with respect to the undeformed state and those defined with respect to the pre-stretched state.

In the solution below, ξ is the dimensionless amplitude of the lead term in the perturbation expansion of sinusoidal surface tractions and displacements. Displacements are normalized by the only length parameter in the problem, the wavelength ℓ of the period in x_1 . The expansion developed in the Appendix and given below is symmetric with respect to $x_1 = 0$. It is exact to order ξ^2 . The displacements and tractions at the surface are

$$\begin{aligned}
U_1 &= (\ell / 2\pi) \left[\xi \hat{u}_1^{(1)} \sin(2\pi x_1 / \ell) + \xi^2 \hat{u}_1^{(2)} \sin(4\pi x_1 / \ell) \right] \\
U_2 &= (\ell / 2\pi) \left[\xi \hat{u}_2^{(1)} \cos(2\pi x_1 / \ell) + \xi^2 \left(\hat{u}_2^{(2)} \cos(4\pi x_1 / \ell) - \hat{u}_1^{(1)} \hat{u}_2^{(1)} / (2\lambda_1) \right) \right] \\
T_1 &= \mu_S \left[\xi \hat{t}_1^{(1)} \sin(2\pi x_1 / \ell) + \xi^2 \hat{t}_1^{(2)} \sin(4\pi x_1 / \ell) \right] \\
T_2 &= \mu_S \left[\xi \hat{t}_2^{(1)} \cos(2\pi x_1 / \ell) + \xi^2 \hat{t}_2^{(2)} \cos(4\pi x_1 / \ell) \right]
\end{aligned} \qquad (8)$$

For prescribed displacements on the surface, the four dimensionless amplitude factors $\hat{u}_\alpha^{(1)}$ and $\hat{u}_\alpha^{(2)}$ can be prescribed arbitrarily, as long they are independent of ξ and at least one of the first order components $\hat{u}_\alpha^{(1)}$ is nonzero. The term $\hat{u}_1^{(1)} \hat{u}_2^{(1)} / (2\lambda_1)$ in the second order contribution to U_2 arises owing to the incompressibility constraint. Alternatively, for prescribed surface

tractions, the four factors $\hat{t}_\alpha^{(1)}$ and $\hat{t}_\alpha^{(2)}$ can be prescribed arbitrarily if at least one of the first order components $\hat{t}_\alpha^{(1)}$ is nonzero.

The amplitude factors in (8) are related by

$$\hat{t}_\alpha^{(1)} = C_{\alpha\beta}(r)\hat{u}_\beta^{(1)}, \quad \hat{t}_\alpha^{(2)} = 2C_{\alpha\beta}(r)\hat{u}_\beta^{(2)} - \frac{1}{\lambda_1}C_{\alpha\beta\gamma}(r)\hat{u}_\beta^{(1)}\hat{u}_\gamma^{(1)} \tag{9}$$

or, in inverted form, by

$$\hat{u}_\alpha^{(1)} = D_{\alpha\beta}(r)\hat{t}_\beta^{(1)}, \quad \hat{u}_\alpha^{(2)} = \frac{1}{2}D_{\alpha\beta}(r)\hat{t}_\beta^{(2)} + \frac{1}{2\lambda_1}D_{\alpha\beta\gamma}(r)\hat{t}_\beta^{(1)}\hat{t}_\gamma^{(1)} \tag{10}$$

Here,

$$C_{\alpha\beta} = \begin{pmatrix} r+1 & 1-r \\ 1-r & r^{-1}(r+1) \end{pmatrix} \tag{11}$$

$$D_{\alpha\beta} = C_{\alpha\beta}^{-1} = \frac{1}{(1+r+3r^2-r^3)}\begin{pmatrix} r+1 & r(r-1) \\ r(r-1) & r(r+1) \end{pmatrix} \tag{12}$$

The six coefficients, $C_{\alpha\beta\gamma} = C_{\alpha\gamma\beta}$, which depend only on $r = \lambda_2/\lambda_1$, have not been obtained analytically but they have been computed to high accuracy (Appendix) and are plotted in Fig. 2 and listed in Table 1. The other set of coefficients is given by $D_{\alpha\beta\gamma} = D_{\alpha\gamma\beta} = D_{\alpha\mu}D_{\beta\nu}D_{\gamma\kappa}C_{\mu\nu\kappa}$.

The relations above are valid for any pre-stretch having $r < 3.383$. The matrices C and D are singular for $r = r_{Biot} \equiv 3.383$ (i.e., when $1+r+3r^2-r^3 = 0$). This is Biot's bifurcation condition for surface wrinkling of a traction-free neo-Hookean half-space (Biot, 1963). Reference will be made later to the Biot condition and to the condition for finite amplitude surface creasing at $r = r_{crease} \equiv 2.38$ (Hohlfeld & Mahadevan, 2011; Hong et al. 2009).

The solution is readily converted to variables defined relative to the pre-stretched state. With the replacements $x_1 \to \bar{x}_1/\lambda_1$, $\ell \to \bar{\ell}/\lambda_1$, $T_\alpha \to \lambda_1\lambda_3\bar{T}_\alpha$ and $\mu_S \to \mu_S/\lambda_3$ in (8), the expansion in the pre-stretched state has the general form

$$U_1 = (\overline{\ell} / 2\pi)\left[\overline{\xi}\hat{u}_1^{(1)} \sin(2\pi\overline{x}_1 / \overline{\ell}) + \overline{\xi}^2\hat{u}_1^{(2)} \sin(4\pi\overline{x}_1 / \overline{\ell})\right]$$

$$U_2 = (\overline{\ell} / 2\pi)\left[\overline{\xi}\hat{u}_2^{(1)} \cos(2\pi\overline{x}_1 / \overline{\ell}) + \overline{\xi}^2\left(\hat{u}_2^{(2)} \cos(4\pi\overline{x}_1 / \overline{\ell}) - \hat{u}_1^{(1)}\hat{u}_2^{(1)} / 2\right)\right]$$

$$\overline{T}_1 = (\mu_S / \lambda_3)\left[\overline{\xi}\hat{t}_1^{(1)} \sin(2\pi\overline{x}_1 / \overline{\ell}) + \overline{\xi}^2\hat{t}_1^{(2)} \sin(4\pi\overline{x}_1 / \overline{\ell})\right]$$

$$\overline{T}_2 = (\mu_S / \lambda_3)\left[\overline{\xi}\hat{t}_2^{(1)} \cos(2\pi\overline{x}_1 / \overline{\ell}) + \overline{\xi}^2\hat{t}_2^{(2)} \cos(4\pi\overline{x}_1 / \overline{\ell})\right]$$

$$(13)$$

The connections now become

$$\hat{t}_\alpha^{(1)} = C_{\alpha\beta}(r)\hat{u}_\beta^{(1)}, \quad \hat{t}_\alpha^{(2)} = 2C_{\alpha\beta}(r)\hat{u}_\beta^{(2)} - C_{\alpha\beta\gamma}(r)\hat{u}_\beta^{(1)}\hat{u}_\gamma^{(1)} \tag{14}$$

$$\hat{u}_\alpha^{(1)} = D_{\alpha\beta}(r)\hat{t}_\beta^{(1)}, \quad \hat{u}_\alpha^{(2)} = \frac{1}{2}D_{\alpha\beta}(r)\hat{t}_\beta^{(2)} + \frac{1}{2}D_{\alpha\beta\gamma}(r)\hat{t}_\beta^{(1)}\hat{t}_\gamma^{(1)} \tag{15}$$

with no changes in the $C's$ and $D's$. There is no explicit λ_1-dependence in the second order contributions when the pre-stretched state is employed.

To illustrate pre-stretch influence on nonlinear substrate traction-deflection behavior, two limiting cases are presented which have relevance to film wrinkling. The representation in the pre-stretched state is employed and a pure sinusoidal normal traction is imposed on the surface of the substrate:

$$\overline{T}_2(x_1) = \overline{T}_2(0)\cos(2\pi\overline{x}_1 / \overline{\ell}), \text{ i.e., } \xi\hat{t}_2^{(1)} = \overline{T}_2(0) / (\mu_S / \lambda_3), \quad \hat{t}_2^{(2)} = 0 \tag{16}$$

Case 1 has no tangential traction constraint: $\overline{T}_1 = 0$ ($\hat{t}_1^{(1)} = 0$, $\hat{t}_1^{(2)} = 0$). Case 2 has tangential displacement constraint, $U_1 = 0$, such that $\hat{t}_1^{(1)} = -D_{12}\hat{t}_2^{(1)} / D_{11}$ and $\hat{t}_1^{(2)} = D_{1\beta\gamma}\hat{t}_\beta^{(1)}\hat{t}_\beta^{(1)} / D_{11}$. In both cases, the normal displacement, $U_2(x_1)$ is given by the second equation in (13) where $\hat{u}_2^{(1)}$ and $\hat{u}_2^{(2)}$ are expressed in terms of $\hat{t}_\alpha^{(1)}$ and $\hat{t}_\alpha^{(2)}$ by (15).

A dimensionless relation between the normal displacement at $\overline{x}_1 = 0$, $U_2(0)$, and the corresponding normal traction amplitude is obtained for the cases prescribed above:

$$\frac{U_2(0)}{\overline{\ell}} = \left(\frac{\overline{T}(0)}{2\pi\mu_S / (\overline{D}_{22}\lambda_3)}\right) - K\left(\frac{\overline{T}(0)}{2\pi\mu_S / (\overline{D}_{22}\lambda_3)}\right)^2 \tag{17}$$

For Case 1, $\bar{D}_{22} = D_{22}$ and $K = \pi \left(D_{222} - D_{12}D_{22} \right) / D_{22}^{\,2}$; for Case 2, $\bar{D}_{22} = (D_{22} - D_{12}^{\,2} / D_{11})$ and

$$K = \pi \frac{\left[\left(D_{211} + \dfrac{D_{12}}{D_{22}} D_{111} \right) \left(\dfrac{D_{12}}{D_{11}} \right)^2 - 2 \left(D_{212} + \dfrac{D_{12}}{D_{22}} D_{112} \right) \left(\dfrac{D_{12}}{D_{11}} \right) + \left(D_{222} + \dfrac{D_{12}}{D_{22}} D_{122} \right) \right]}{\bar{D}_{22}^{\,2}}$$

For the normalization used in (17), the coefficient characterizing the lowest order influence of nonlinearity, K, depends on pre-stretch only through r for both cases. This dependence is plotted in Fig. 3, which makes clear the significant effect of both the pre-stretch and the tangential constraint. The normalized traction-displacement relation (17) is plotted in Fig. 4 for several values of pre-stretch for Case 1.

The plots in Figs. 3 and 4 reveal important aspects of the role of pre-stretch on substrate nonlinearity. A nonlinear softening or stiffening response depends on the pre-stretch only through $r = \lambda_2 / \lambda_1 = 1 / \lambda_1^2 \lambda_3$. If $r < 1$, softening occurs for upward deflections and stiffening occurs for downward deflections. Conversely, $r > 1$ produces stiffening for upward deflections and softening for downward deflections. The coefficient K vanishes if $r = 1$ corresponding to no pre-stretch. Thus, the lowest order nonlinearity without pre-stretch is cubic while otherwise it is quadratic. These same trends hold for Case 2 with tangential displacements constrained to be zero. For plane strain, $\lambda_3 = 1$, pre-compression ($\lambda_1 < 1$) results a stiffening response for upward deflections and a softening response for downward deflections; pre-tension ($\lambda_1 > 1$) has the opposite effect. These trends for plane strain are in accord with earlier observations based on the finite element calculations of Zang et al. (2012).

3. Stiff films on linearized pre-stretched substrates

To set the stage for the present study, it is useful to summarize the wrinkling behavior of very stiff linear elastic films bonded to compliant, but linear, elastic substrates. Allen (1969) presented one of the earliest analyses of these systems with the film modeled by nonlinear plate theory and the substrate taken to be a linear elastic half-space. Recent work relevant to the present study has extended such analyses by accounting for the effect of pre-stretch of neo-

Hookean substrates on the linearized stiffness of the half-space (Sun, et al. 2012; Cao & Hutchinson 2012a), and it is this work that will be summarized.

If the film is assumed to constrain the tangential displacement of the substrate to be zero, then the linearized response of a neo-Hookean substrate to a sinusoidal normal displacement, $U_2 = U_2(0)\cos(2\pi\bar{x}_1 / \bar{\ell})$, is $\bar{T}_2 = \bar{T}_2(0)\cos(2\pi\bar{x}_1 / \bar{\ell})$, where from the results of the previous section, $\bar{T}_2(0) = 2\pi\left(\mu_S / \lambda_3\right)C_{22}(r)\left(U_2(0) / \bar{\ell}\right)$. The barred quantities are defined with respect to the pre-stretched state of the substrate. This provides the linearized stiffness of the half-space in the model as dependent on the substrate pre-stretch specified by μ_S / λ_3 and $r = 1/\lambda_1^2\lambda_3$. An unstretched film of thickness h is bonded to the pre-stretched substrate and, subsequently, the film/substrate system is subject to plane strain compression. For an incompressible film with elastic shear modulus, μ_F, the compressive strain in the film at bifurcation and the wavelength of the critical mode are:

$$\varepsilon_C = \frac{1}{4}\left(\frac{3\mu_S}{2\lambda_3\mu_F}\left(1+r^{-1}\right)\right)^{2/3} \quad \text{and} \quad \bar{\ell}_C = 2\pi h\left(\frac{3\mu_S}{2\lambda_3\mu_F}\left(1+r^{-1}\right)\right)^{-1/3} \tag{18}$$

These formulas accurately capture the effect of pre-stretch on bifurcation for film/substrate stiffness ratios satisfying $\lambda_3\mu_F / \mu_S \geq 100$ (Cao & Hutchinson 2012a).

The post-bifurcation problem for the model with a fully nonlinear von Karman plate on the linear substrate can be solved exactly in closed form (Chen & Hutchinson 2004). The shape and wavelength of the vertical deflection of the film in the bifurcation mode, $U_2 = \xi h\cos(2\pi\bar{x}_1 / \bar{\ell}_C)$, do not change as ε increases above ε_C, and the dimensionless amplitude of the mode increases as

$$\xi = \sqrt{\frac{\varepsilon}{\varepsilon_C} - 1} \quad \text{or} \quad \varepsilon = \varepsilon_C\left(1 + \xi^2\right) \tag{19}$$

The post-bifurcation behavior is highly stable according to this model with the deflection increasing monotonically (19) as the compression is increased. The results, (18) and (19), which

9

are limited to large $\lambda_3 \mu_F / \mu_S$ and, thus, relatively small ε, will be compared with exact results for a neo-Hookean bilayer in the next section.

4. Initial post-wrinkling behavior of a neo-Hookean bilayer

In this section, wrinkling of a thin neo-Hookean film bonded to a deep compliant neo-Hookean substrate is studied for films attached to substrates that have been pre-stretched. The film/substrate system is then subject to plane strain compression. The stability and initial evolution of the wrinkling mode is investigated using an initial post-bifurcation analysis along the lines originally formulated by Koiter (Koiter 1945; van der Heijden 2009) and further developed and promulgated by Thompson (1963) and Thompson and Hunt (1973) for a wide class of elastic systems. The primary focus will be on the stability of the wrinkling bifurcation and the evolution of the wrinkling mode shape immediately following bifurcation in the range when the perturbation expansion retains its accuracy.

The substrate is semi-infinite with ground state modulus μ_S. The film has initial thickness, h, with ground state modulus μ_F. Attention is limited to systems with $\mu_F > \mu_S$. The uniform pre-stretch in the substrate is now denoted by $(\lambda_1^0, \lambda_2^0, \lambda_3^0)$, and the unstretched film is bonded to the substrate in this state. Following film attachment, the system is subject to a uniform plane strain compression by imposing a compressive strain in the 1-direction, ε, with no additional straining in the out-of-plane direction. The top surface of the film is traction-free. The fundamental solution characterizing the pre-bifurcation state has uniform stretches in the film and in the substrate. With λ_i^F denoting the stretches in the film in the fundamental solution relative to its unstretched state, the imposed nominal overall compressive strain is $\varepsilon \equiv -\left(\lambda_1^F - 1\right)$. With λ_i^S denoting the stretches in the substrate in the fundamental solution relative to its undeformed state, the following dependencies on ε hold:

$$\lambda_1^F = 1-\varepsilon, \ \lambda_2^F = 1/(1-\varepsilon), \ \lambda_3^F = 1 \quad \text{with} \ r_F = 1/(1-\varepsilon)^2 \tag{20}$$

$$\lambda_1^S = \lambda_1^0(1-\varepsilon), \ \lambda_2^S = \lambda_2^0/(1-\varepsilon), \ \lambda_3^S = \lambda_3^0 \ \text{with} \ r_S = r_S^0/(1-\varepsilon)^2 \tag{21}$$

where $r_S^0 = \lambda_2^0 / \lambda_1^0 = 1/\lambda_1^{02}\lambda_3^0$.

10

Two sets of Lagrangian coordinates are used, one for the film and the other for the substrate. Each is defined with respect to the undeformed state in that layer, and each will be denoted by x_i, but due regard will be made for the difference in definition from one layer to the other owing to the fact that the substrate is pre-stretched. In each layer, the 3-coordinate lies in the out-of-plane direction and $x_2 = 0$ coincides with the film-substrate interface. The periodic bifurcation and post-bifurcations solutions sought have the form

$$u_1 = (\lambda_1 - 1)x_1 + U_1(x_1, x_2), \quad u_2 = (\lambda_2 - 1)x_2 + U_2(x_1, x_2), \quad u_3 = (\lambda_3 - 1)x_3 \tag{22}$$

where the stretches in each layer are given by (20) or (21) and the coordinate definition switches from layer to layer. The fundamental solution is given with $\mathbf{U} = 0$ and it is fully characterized by the substrate pre-stretches, λ_i^0, and the overall compressive strain, ε.

The energy change in the film/substrate system from that in the fundamental solution (now defined per wavelength per unit x_3 in the film) is

$$\Phi(\lambda_i^0, \varepsilon, \mathbf{U}, Q) = \mu_F \int_0^{\ell_F} \int_0^h I(\lambda_i^F, \mathbf{U}, Q) dx_2 dx_1 + (\mu_S / \lambda_3^0) \int_0^{\ell_S} \int_{-\infty}^0 I(\lambda_i^S, \mathbf{U}, Q) dx_2 dx_1 \tag{23}$$

Here, I is defined in (3), with due regard for variable changes from layer to layer; ℓ_F and $\ell_S = \ell_F / \lambda_1^0$ are the period wavelengths in the respective coordinate systems.

The detailed bifurcation and initial post-bifurcation analysis is presented in the Appendix. The central findings obtained from the perturbation expansion about the critical strain at bifurcation, ε_C, will be presented in this section. The vertical deflection of the upper surface of the film is

$$\frac{U_2}{h} = \xi \cos\left(\frac{2\pi x_1}{\ell_F}\right) + \xi^2 \left[\hat{u}_2^{(2)} \cos\left(\frac{4\pi x_1}{\ell_F}\right) + \hat{u}_0^{(2)} \right] \tag{24}$$

and the relation between the dimensionless mode amplitude, ξ, and the overall imposed compressive strain is

$$\varepsilon = \varepsilon_C \left(1 + b\xi^2\right) \tag{25}$$

The expansions are exact to order ξ^2; higher order terms are not listed. Using variable changes similar as those discussed for the substrate in Section 2, it can be shown that ε_C, ℓ_F / h, b, $\hat{u}_0^{(2)}$ and $\hat{u}_2^{(2)}$ depend only on two dimensionless parameters:

$$r_S^0 = \frac{\lambda_2^0}{\lambda_1^0} = \frac{1}{(\lambda_1^0)^2 \lambda_3^0}, \quad \mu_R = \frac{\mu_S}{\lambda_3^0 \mu_F} \tag{26}$$

The reduction in the number of essential parameters makes it possible to present relatively complete results for all combinations of moduli and pre-stretch.

The critical strain, ε_C, and the normalized wavelength, ℓ_F / h, are presented in Fig. 5 as a function of $\lambda_3 \mu_F / \mu_S$ for four values of r_S^0. These results are in complete agreement with the results for plane strain pre-stretch presented by Cao & Hutchinson (2012a) who did not note the parametric dependence reduction allowed by (26). More extensive results for the bifurcation problem have been presented in that reference with comparisons to (18) from the simpler model in Section 3.

The initial post-bifurcation coefficient, b, governing the relation between the mode amplitude and the imposed compression in (25) is plotted in Fig. 6. By (19), the simpler model for a stiff film on a linear substrate predicts $b = 1$. For $\lambda_3 \mu_F / \mu_S > 100$, the fully nonlinear results for b in Fig. 6 are only slightly below unity, and thus the initial post-bifurcation expansion confirms the simpler model's prediction that the wrinkling bifurcation is stable for sufficiently large $\lambda_3 \mu_F / \mu_S$. Complete agreement between the two predictions should not be expected, even asymptotically for large $\lambda_3 \mu_F / \mu_S$, because, not only does the simpler model not account for substrate nonlinearity, it does not fulfill all the conditions on continuity across the film/substrate interface.

As seen in Fig. 6, b decreases for smaller $\lambda_3 \mu_F / \mu_S$ and can become negative. Bifurcation is unstable if $b < 0$. As depicted in bifurcation plot in Fig. 7, if $b < 0$, no wrinkling solution exists in the vicinity of the bifurcation point when the imposed compressive strain is increased above ε_C. A perfect film/substrate system having $b < 0$ becomes unstable when ε

attains ε_C and would snap dynamically into a finite amplitude wrinkling mode, which the present perturbation analysis cannot predict. Included in Fig. 7 is a plot of the boundary between stable and unstable bifurcation in the parameter plane $\left(r_S^0, 1/\mu_R \right)$. Over most of the parameter range considered in this paper, bilayer wrinkling is stable in the initial post-bifurcation regime. Unstable wrinkling bifurcation is predicted only when the modulus parameter, $\lambda_3 \mu_F / \mu_S$, is less than about 5. Tensile pre-stretch of the substrate ($r_S^0 < 1$) can suppress the bifurcation instability. With no pre-stretch ($r_S^0 = 1$), bifurcation is unstable only for $\lambda_3^0 \mu_F / \mu_S < 1.73$. Nevertheless, sharply reduced values of b occur for $\lambda_3 \mu_F / \mu_S < 10$, especially if the substrate is subject to pre-compression with $r_S^0 \geq 1$. Reduced values of b imply that wrinkles develop more rapidly as the overall compression is increased above ε_C.

The film in this study experiences plane strain deformation. For the entire set of parameters for which results have been presented in this paper, the compressive strain at bifurcation in the film, ε_C, is below the strain required for the existence of finite amplitude crease, $\varepsilon_{crease} = 0.35$, and well below the Biot strain for surface wrinkles, $\varepsilon_{Biot} = 0.458$. The wavelength of bifurcation mode in all cases is many times the film thickness (c.f., Fig. 5), and the mode has no resemblance to a crease or a short wavelength Biot surface mode within the film. It is also true that in all cases the essential stretch ratio in the substrate at bifurcation, $r_S = \lambda_2^S / \lambda_1^S = r_S^0 / (1-\varepsilon)^2$, never exceeds $r_{Biot} = 3.383$ corresponding to a singular substrate stiffness matrix as discussed in Section 2. However, r_S does exceed $r_{crease} = 2.38$ when $\lambda_3 \mu_F / \mu_S$ is sufficiently small for pre-stretch with $r_S^0 > 1$. This is illustrated in Fig. 8 where the values of r_F and r_S at bifurcation are plotted as a function of $\lambda_3 \mu_F / \mu_S$ for values of r_S^0 corresponding to the instability boundary in Fig. 7. While the film ratio, r_F, is always below r_{crease}, the substrate ratio, r_S, exceeds r_{crease} on most of the instability boundary. The implications of $r_S > r_{crease}$ are not obvious. As long as $r_S < r_{Biot}$, the analysis carried out here is well behaved. However, if $r_{crease} < r_S < r_{Biot}$, it is possible that energetically favorable finite amplitude crease-like modes for the bilayer may exist at compressive strains below the bifurcation strain predicted here. If so, these modes would not emerge as a bifurcation but would

have to be triggered by an initial imperfection. In their analysis, Hohlfeld and Mahadevan (2011) attached to the substrate a very thin film having bending stiffness but no stretching stiffness to regularize the substrate crease problem. The fact that these authors find crease modes when the film bending stiffness is sufficient small suggests that there may be a range of $\lambda_3 \mu_F / \mu_S$ for which such finite amplitude crease-like modes may supersede wrinkling for the bilayer. It is also possible that the bilayer system snaps into a crease-like mode in the regime when bifurcation is unstable. The existence of these modes is beyond the scope of this study.

The evolution of the shape of the wrinkle after bifurcation is determined by (24) and, specifically, by $\hat{u}_2^{(2)}$, which is plotted in Fig. 9. For $\lambda_3 \mu_F / \mu_S \geq 100$, $\hat{u}_2^{(2)}$ is relatively small and positive. However, for sufficiently small $\lambda_3 \mu_F / \mu_S$, $\hat{u}_2^{(2)}$ changes sign and becomes increasing negative as $\lambda_3 \mu_F / \mu_S$ decreases, depending strongly on the pre-stretch parameter, r_S^0. The influence of $\hat{u}_2^{(2)}$ on the wrinkle shape evolution is illustrated in Fig. 10. A positive $\hat{u}_2^{(2)}$, which is promoted by large $\lambda_3 \mu_F / \mu_S$ and pre-stretch with $r_S^0 < 1$, gives rise to amplification of the wrinkle peaks and a flattening of the valleys. This is in accord with softening for upward deflections and stiffening deflections noted in Section 2 for the nonlinear behavior of the substrate when $r_S < 1$. Conversely, negative $\hat{u}_2^{(2)}$, which is promoted by smaller $\lambda_3 \mu_F / \mu_S$ and pre-stretch with $r_S^0 > 1$, gives rise to flattening of the peaks and sharpening of the valleys. This, again, is in accord with the expectation noted in Section 2 for substrates with $r_S > 1$. Thus, the initial post-bifurcation analysis points to the possibility of the wrinkling mode evolving towards either ridges when $\hat{u}_2^{(2)} > 0$ or folds when $\hat{u}_2^{(2)} < 0$. Ridges (Cao & Hutchinson 2012a; Zang et al. 2012; Ebata et al. 2012) and folds (Brau et al. 2010; Sun et al. 2012) are advanced post-buckling modes that form at compressive strains that can be many times ε_C and well outside the range of validity of the perturbation expansions developed here. Nevertheless, the tendency towards the two types of advanced modes is evident in the perturbation of the sinusoidal bifurcation mode. Moreover, this tendency is in general agreement with the role of stretch on the nonlinear response of the substrate obtained in Section 2.

5. Conclusions

Two dimensionless parameters characterize the solutions for the neo-Hookean bilayer system: a measure of substrate pre-stretch, $r_S^0 = \lambda_2^0 / \lambda_1^0 = 1 / \lambda_1^{0\,2} \lambda_3^0$, and a stretch modified modulus ratio, $\mu_R = \mu_S / \lambda_3^0 \mu_F$. For $\mu_R < 0.1$, the compressive strain in the film at bifurcation is less than 0.1 and the wrinkling bifurcation is stable, in agreement with the classical model for wrinkling of stiff films on compliant linear substrates. However, when the film stiffness is more comparable to that of the substrate, with $0.2 < \mu_R < 0.5$, bifurcation can be unstable, especially for compressive pre-stretches having $r_S^0 > 1$. Over the entire range of bifurcations investigated here the wrinkling mode at bifurcation has a wavelength that is very long compared to the film thickness. Moreover, the compressive strains in the film are well below both the short-wavelength Biot surface wrinkling strain and the critical strain for existence of a finite amplitude surface crease within the film. For compressive pre-stretch, $r_S^0 > 1$, in the modulus range $0.2 < \mu_R < 0.5$, the compressive strain within the substrate can exceed the critical strain for a finite amplitude surface crease. It remains an open question whether the bilayer will experience imperfection-driven finite amplitude creasing modes below the bifurcation strain in this range.

The classical model for stiff films on compliant linear substrates predicts that the wrinkling mode remains stable with no change from the sinusoidal shape under plane strain compression. It is substrate nonlinearity that influences both the stability of wrinkling and the evolution of the shape of the wrinkling mode as the compression is increased beyond the onset of bifurcation. Substrate pre-stretch has been shown to have a strong effect on substrate nonlinearity. Compression, with $r_S^0 > 1$, gives rise to nonlinearity which favors deflections into the substrate over outward deflections, while tensile pre-stetch, with $r_S^0 < 1$, has the opposite effect. The former favors evolution towards fold-like wrinkle shapes while the latter favors evolution towards ridge-like shapes. The details of these conclusions are based on the assumption of neo-Hookean elasticity but the general trends are likely to carry over to more elaborate nonlinear elastic material models.

The initial post-bifurcation expansion does not reveal the unusual wrinkling modes observed at compressive strains well above the bifurcation strain such as period doubling and

folding (Pocivavsek et. al. 2008, Brau et al. 2011; Sun et al. 2012; Cao & Hutchinson 2012a) and ridging (Ebata et al. 2012; Zang, et al. 2012). The transition of a periodic wrinkle pattern into a pattern that alternates between highly localized undulations and relatively flat regions is also a consequence of substrate nonlinearity (Hunt et al. 1989; Wadee et al. 1997; Zang et al. 2012). The perturbation approach in the present study which employs the sinusoidal bifurcation mode as the leading term brings in the higher order harmonics of this mode. While it can reveals some effects of substrate nonlinearity, it is not able to capture localization phenomena such as folding or ridging.

References

Allen, H. G. 1969 *Analysis and design of sandwich panels*. Pergamon Press, New York.

Biot, M.A. 1963 Surface instability of rubber in compression. *Appl. Sci. Res*. **12**, 168-182.

Brau, F., Vandeparre, H., Sabbah, A., Poulard, C., Boudaoud, A., & Damman, P. 2010. Multiple-length-scale elastic instability mimics parametric resonance of nonlinear oscillators. *Nat. Phys*. **7**, 56-60.

Cai, Z. & Fu, Y. 1999 On the imperfection sensitivity of a coated elastic half-space. *Proc. R. Soc. A*. **455**, 3285-3309.

Cao, Y. & Hutchinson, J. W. 2012a Wrinkling phenomena in neo-Hookean film/substrate systems. *J. Appl. Mech*. **79**, 031019-1-9.

Cao, Y. & Hutchinson, J. W. 2012b From wrinkles to creases in elastomers: the instability and imperfection-sensitivity of wrinkling. *Proc. R. Soc. A*. **468**, 94-115.

Chan, E.P. & Crosby, A.J. 2006 Spontaneous formation of stable aligned wrinkle patterns. *Soft Matter* **2**, 324-328.

Chen, X. & Hutchinson, J.W. 2004. Herringbone buckling patterns of compressed thin films on compliant substrates. *J. Appl. Mech*. 71, 597-603.

Ebata, Y., Croll, A.B. & Crosby, A.J. 2012 Wrinkling and strain localizations in polymer thin films. *Soft Matter* **8**, 9086-9091.

Genzer, J. & Groenewold, J. 2006 Soft matter with hard skin: From skin wrinkles to templating and material characterization. *Soft Matter* **2**, 310-323.

Hohlfeld, E.B. & Mahadevan, L. 2011 Unfolding the sulcus. *Phys. Rev. Letters* **106**, 105702-1-4.

Hong, W., Zhao, X. & Suo, Z. 2009 Formation of creases on the surfaces of elastomers and gels. *App. Phys. Letters* **95**, 111901-1-3.

Hunt, G. W., Bolt, H. M. &Thompson, J. M. T. 1989 Structural localization phenomena and the dynamical phase-space analogy. *Proc. R. Soc. A* **425**, 245-267.

Koiter, W.T. 1945 *On the stability of elastic equilibrium* (in Dutch with English summary). Thesis Delft, H.J. Paris, Amsterdam. An English translation is available online: http://imechanica.org/node/1400 .

Li, B., Cao, Y-P., Feng, X-Q. & Gao, H. 2012 Mechanics of morphological instabilities and surface wrinkling in soft materials: a review. *Soft Matter* **8**, 5728-5745.

Pocivavsek, L., Dellsy, R., Kern, A., Johnson, S., Lin, B., Lee, K.Y.C. & Cerda, E. 2008 Stress and Fold Localization in Thin Elastic Membranes. *Science* **320**, 912-916.

Sun, J-Y., Xia, S., Moon, M-Y., Oh, K.H., & Kim, K-S. 2012 Folding wrinkles of a thin stiff layer on a soft substrate. *Proc. Roy. Soc. A* **468**, 932-953.

Thompson, J.M.T. 1963 Basic principles in the general theory of elastic stability. *J. Mech. Phys. Solids* **11***, 13-25.

Thompson, J.M.T. & Hunt, G.W. 1973 *A general theory of elastic stability.* John Wiley & Sons, London.

van der Heijden, A.M. 2009 *W.T. Koiter's elastic stability of solids and structures*. Cambridge, UK: Cambridge University Press.

Wadee, M. K., Hunt, G. W. & Whiting, A. I. M. 1997 Asymptotic and Rayleigh-Ritz routes to localized buckling solutions in an elastic instability problem. *Proc. R. Soc.A* **453**, 2085-2107.

Yin, J., Cao, Z., Li, C., Sheinman, I & Chen, X. 2008 Stress-driven buckling patterns in spheroidal core/shell structures. *PNAS* **105**, 19132-19135.

Yin, J., Yaguer, J.L., Eggenspieler, D., Gleason, K.K. & Boyce, M.C. 2012 Deterministic order in surface micro-topologies through sequential wrinkling. *Adv. Mat.* **24**, 5441-5446.

Zang, J., Zhao, X., Cao, Y. & Hutchinson, J.W. 2012 Localized ridge wrinkling of stiff films on compliant substrates. *J. Mech. Phys. Solids* **60**, 1265-1279.

Appendix

Nonlinear behavior of pre-stretched neo-Hookean half-space

In the notation of (8), the solution to the linearized equations in (4)-(7) is

$$\left. \begin{array}{l} \left(U_1^{(1)},U_2^{(1)},\lambda_1 Q^{(1)}\right) = \xi k^{-1}\left(f(\zeta)\sin kx_1, g(\zeta)\cos kx_1, k\,q(\zeta)\cos kx_1\right) \\[4pt] f = -c_1 e^{r\zeta} - c_2 r^1 e^{\zeta}, \;\; g = c_1 e^{r\zeta} + c_2 e^{\zeta}, \;\; q = c_1(r - r^{-1})e^{r\zeta} \\[4pt] c_1 = -(r-1)^{-1}\left(r\hat{u}_1^{(1)} + \hat{u}_2^{(1)}\right), \;\; c_2 = r(r-1)^{-1}\left(\hat{u}_1^{(1)} + \hat{u}_2^{(1)}\right) \end{array} \right\} \tag{A-1}$$

with $k = 2\pi / \ell$ and $\zeta = kx_2$. From this solution, and using the linearized relation (7) for the surface tractions, one obtains the relations of order ξ in Section 2.

The next step in the perturbation solution is to substitute an expansion in the general form of (8) into the nonlinear equations (4)-(7) and require all terms of order ξ^2 to vanish. The second order solution is

$$\begin{aligned} \left(U_1^{(2)},U_2^{(2)},\lambda_1 Q^{(2)}\right) &= \frac{\xi^2 k^{-1}}{2\lambda_1}\left(0, G_0(\zeta), k\,H_0(\zeta)\right) + \\[4pt] &\quad \frac{\xi^2 k^{-1}}{2\lambda_1}\left(F(\zeta)\sin 2kx_1, G(\zeta)\cos 2kx_1, k\,H(\zeta)\cos 2kx_1\right) \end{aligned} \tag{A-2}$$

where $G_0 = -f\,g$, $H_0 = -(f\,g)' - f\,q$, and F, G and H satisfy the 4th order ode system

$$F'' - 4F + 2rH = g\,q' - g'\,q, \;\; G'' - 4G - H' = f\,q' - f'\,q, \;\; G' + 2rF = f'\,g - f\,g' \tag{A-3}$$

with $(\ )' = d(\ )/d\zeta$. The boundary conditions for the 4$^{\text{th}}$ order system of ode's (A-3) require the functions to vanish as $\zeta \to -\infty$ and $\left(F(0), G(0)\right) = 2\lambda_1\left(\hat{u}_1^{(2)}, \hat{u}_2^{(2)}\right)$. The second order surface traction coefficients in (8) are determined from (7) as

$$\hat{t}_1^{(2)} = \left(2\lambda_1\right)^{-1}\left(F' - g\,q\right)_{\zeta=0}\ ,\ \hat{t}_2^{(2)} = \left(2\lambda_1\right)^{-1}\left(G' - H - f\,q\right)_{\zeta=0} \tag{A-4}$$

The solution to the problem can be constructed as the sum of a homogeneous solution, with $f = g = q = 0$ in (A-3) and (A-4), satisfying $\left(F(0), G(0)\right) = 2\lambda_1\left(\hat{u}_1^{(2)}, \hat{u}_2^{(2)}\right)$ and a particular solution, with f, g and h as defined in (A-1), and $F(0) = G(0) = 0$. The homogeneous solution gives the contribution, $\hat{t}_\alpha^{(2)} = 2C_{\alpha\beta}\hat{u}_\beta^{(2)}$, in (9) while particular solution provides the other part. In principle, it is possible to produce a closed form analytical solution to the particular problem, but the algebraic effort would be prohibitive. Instead, in computing the values of $C_{\alpha\beta\gamma}$ given in Table 1, the ode system is solved numerically and the coefficients are identified using (A-4).

Given that the displacements decay exponentially to zero as $\zeta \to -\infty$ and that the material is incompressible, displacements imposed on the surface cannot change the volume of the half-space. This condition can be expressed as $\int_0^\ell \left(U_2\left(\lambda_1 + dU_1/dx_1\right)\right)_{x_2=0} dx_1 = 0$. It is not necessary to impose this condition as an extra condition because the solution satisfies (4) ensuring incompressibility to order ξ^2. The second order term in (8), $\xi^2\hat{u}_1^{(1)}\hat{u}_2^{(1)}/(2\lambda_1)$, is a consequence of the incompressibility constraint and it derives from $G_0(0) = -f(0)g(0)$.

Initial post-bifurcation analysis of neo-Hookean bilayer

The nonlinear Euler equations, (4)-(7), listed in Section 2 and expressed in each of the two layers render the energy functional (23) stationary. These govern the plane strain bilayer problem, together with conditions that the tractions and displacements are continuous across the film/substrate interface on $x_2 = 0$ and tractions vanish on the film surface. The linearized equations govern the bifurcation problem. It's solution is given by the following extended recipe:

$$\left(U_1^{(1)}, U_2^{(1)}, \lambda_1 Q^{(1)}\right) = \xi h\left(f(\zeta)\sin kx_1, g(\zeta)\cos kx_1, k\,q(\zeta)\cos kx_1\right) \tag{A-5}$$

where $k \to k_F = 2\pi/\ell_F$ and $\lambda_1 \to \lambda_1^F$ in the film, $x_2 > 0$, and where $k \to k_S = 2\pi/\ell_S$ and $\lambda_1 \to \lambda_1^S$ in the substrate, $x_2 < 0$. The coordinates x_α are different in the film and in the substrate, as defined in Section 4, and $\zeta = kx_2$ changes accordingly from film to substrate. The functions in (A-5) that satisfy the linearized Euler equations are

$$
\begin{aligned}
f &= -c_1 e^{r_F \zeta} - c_2 r_F^{-1} e^{\zeta} + c_3 e^{-r_F \zeta} + c_4 r_F^{-1} e^{-\zeta}, \quad \zeta > 0 \\
&= -c_5 e^{r_S \zeta} - c_6 r_S^{-1} e^{\zeta}, \quad \zeta < 0 \\
g &= c_1 e^{r_F \zeta} + c_2 e^{\zeta} + c_3 e^{-r_F \zeta} + c_4 e^{-\zeta}, \quad \zeta > 0 \\
&= c_5 e^{r_S \zeta} + c_6 e^{\zeta}, \quad \zeta < 0 \\
q &= c_1 (r_F - r_F^{-1}) e^{r_F \zeta} - c_3 (r_F - r_F^{-1}) e^{-r_F \zeta}, \quad \zeta > 0 \\
&= c_5 (r_S - r_S^{-1}) e^{r_S \zeta}, \quad \zeta < 0
\end{aligned}
\right\} \tag{A-6}
$$

with the c_i to be determined.

Continuity of tractions and displacements across $\zeta = 0$ and zero tractions on $\zeta = k_F h$ provide the eigenvalue equation, $M_{ij} c_j = 0$ ($i = 1,6; j = 1,6$), where M is given by

$$
\begin{bmatrix}
-2r_F e^{r_F k_F h} & -(r_F + r_F^{-1})e^{k_F h} & -2r_F e^{-r_F k_F h} & -(r_F + r_F^{-1})e^{-k_F h} & 0 & 0 \\
-(r_F + r_F^{-1})e^{r_F k_F h} & -2e^{k_F h} & (r_F + r_F^{-1})e^{-r_F k_F h} & 2e^{-k_F h} & 0 & 0 \\
-1 & -r_F^{-1} & 1 & r_F^{-1} & 1 & r_S^{-1} \\
1 & 1 & 1 & 1 & -1 & -1 \\
-2r_F & -(r_F + r_F^{-1}) & -2r_F & -(r_F + r_F^{-1}) & 2\mu_R r_S & \mu_R(r_S + r_S^{-1}) \\
-(r_F + r_F^{-1}) & -2 & (r_F + r_F^{-1}) & 2 & \mu_R(r_S + r_S^{-1}) & 2\mu_R
\end{bmatrix}
$$

By (20) and (21), this matrix can be expressed in terms of r_S^0, $\mu_R \equiv \mu_S/(\lambda_3 \mu_F)$, ε and ℓ_F/h. (Note that $k_F h = 2\pi h/\ell_F$. While $k_S = \lambda_1^0 k_F$ depends on λ_1^0, it does not need to be specified in the eigenvalue calculation or in the post-bifurcation calculations below.) The eigenvalue condition for ε is $|M| = 0$. The critical eigenvalue and associated wavelength, ε_C and $(\ell_F/h)_C$, are obtained by minimizing the eigenvalue with respect to the wavelength. The results plotted in Fig. 5 have been obtained numerically. The associated eigenfunction is normalized by requiring $g(0) = 1$ such that on the surface $U_2^{(1)} = \xi h \cos(2\pi x_1/\ell_F)$.

The problem for the second order solution of order ξ^2 is obtained in a manner similar to that described for the substrate problem with the nonlinear equations (4)-(6) governing in the respective regions. Now, however, nonlinear equations (7) governing continuity of tractions across the interface and zero traction on the film surface must also be considered. The second order solution is

$$\left(U_1^{(2)}, U_2^{(2)}, \lambda_1 Q^{(2)}\right) = \frac{\xi^2 k h^2}{2\lambda_1} \left(F_0(\zeta), G_0(\zeta), k\, H_0(\zeta)\right) +$$

$$\frac{\xi^2 k h^2}{2\lambda_1} \left(F(\zeta)\sin 2kx_1, G(\zeta)\cos 2kx_1, k\, H(\zeta)\cos 2kx_1\right) \tag{A-7}$$

where definitions switch from film to substrate in the same manner as in (A-5). The two ode systems are

$$F_0'' = 0,\; G_0'' - H_0' = (fh)',\; G_0' = -(f\,g)' \tag{A-8}$$

$$\left.\begin{aligned} F'' - 4F + 2rH &= gh' - g'h \\ G'' - 4G - H' &= f\,h' - f'\,h \\ G' + 2rF &= f'\,g - f\,g' \end{aligned}\right\} \tag{A-9}$$

The traction-free boundary conditions on the film surface require (on $\zeta = k_F h$)

$$F' - 2r_F G - g\,q = 0,\; G_0' - H_0 - f\,q,\; G' - 2r_F F - H - fq = 0$$

On the interface ($\zeta = 0$), continuity of displacements requires continuity of F_0, F, G_0 and G, while continuity of tractions requires

$$\left(F' - 2r_F G - g\,q\right) = \mu_R \left(F' - 2r_S G - g\,q\right)$$

$$\left(G' - 2r_F F - H - f\,q\right) = \mu_R \left(G' - 2r_S F - H - f\,q\right)$$

$$\left(G_0' - H_0 - f\,q\right) = \mu_R \left(G_0' - H_0 - f\,q\right)$$

with terms evaluated in the film on the left and those in the substrate on the right.

The solution to (A-8) satisfying all the boundary and continuity conditions is

$$F_0 = 0, \ G_0 = -f\,g, \ H_0 = -(f\,g)' - f\,q$$

The solution to the 4$^{\text{th}}$ order system of linear odes, (A-9), has been obtained numerically. The numerical solution has been carried out using a standard ode solver, and, in doing so, it has been useful to recast the system using four dependent variables that are continuous across the interface: F, G, and the combination of variables in the two traction conditions above.

The final step in the calculation is the evaluation of the initial post-bifurcation stability coefficient b defined in (25). One way to compute b would be to continue the perturbation process by deriving the boundary value problem for terms of order ξ^3, and then use b to suppress the secular nonhomogeneous terms. In addition to providing a unifying framework, one of the benefits of the general theory of initial post-bifurcation developed by Koiter (1945) and Thompson & Hunt (1973) is that it yields a general expression for b in terms of the solution to the first and second order perturbations without direct consideration of the third order problem. Here, we present this expression without derivation using a compact notation employed by Cao & Hutchinson (2012b) in a stability analysis of neo-Hookean half-space surface winkling.

With the dependence on pre-stretch, λ_i^0, implicit, represent the energy functional (23) as $\Phi(\varepsilon, U)$ with $U \equiv (U_1, U_2, Q)$. The full solution (22) has the form

$$u = U^{(0)}(\varepsilon) + U = U^{(0)}(\varepsilon) + \xi U^{(1)} + \xi^2 U^{(2)} + \ldots$$

with $U^{(0)}(\varepsilon)$ as the fundamental solution. The formula for b in this compact notation is

$$b\,\varepsilon_C \frac{\partial^3 \Phi(\varepsilon_C, 0) U^{(1)\,2}}{\partial \varepsilon\, \partial^2 U} = -\frac{\partial^3 \Phi(\varepsilon_C, 0) U^{(1)\,2} U^{(2)}}{\partial^3 U} \tag{A-10}$$

Because Φ in (23) has no quartic terms in U, there is no contribution of terms proportional to $U^{(1)\,4}$ in (A-10), as would generally be present. Eq. (A-10) is made explicit in the following:

$$\frac{\partial^3 \Phi\left(\varepsilon_C,0\right)U^{(1)\,2}U^{(2)}}{\partial^3 U} =$$

$$-\int_V \frac{2\mu}{\lambda_1}\left\{\lambda_1 Q^{(1)}\left(U_{1,1}^{(1)}U_{2,2}^{(2)}+U_{2,2}^{(1)}U_{1,1}^{(2)}-U_{1,2}^{(1)}U_{2,1}^{(2)}-U_{2,1}^{(1)}U_{1,2}^{(2)}\right)+\lambda_1 Q^{(2)}\left(U_{1,1}^{(1)}U_{2,2}^{(1)}U_{1,2}^{(1)}U_{2,1}^{(1)}\right)\right\}dV$$

$$=-\frac{2\pi\mu_F k_F^{\;2}h^4}{\lambda_1^{F\,2}}\left\{B_F+\mu_R B_S\right\},\quad B_F=\int_0^{k_F h}F_B(\zeta)d\zeta,\quad B_S=\int_{-\infty}^0 F_B(\zeta)d\zeta,$$

with $F_B = fq(G_0' + G'/2) + g'qF + f'qG + gqF'/2 + H_0(fg)' + H(fg' - f'g)/2$, and

$$\frac{\partial^3 \Phi\left(\varepsilon_C,0\right)U^{(1)\,2}}{\partial\varepsilon\,\partial^2 U}=\int_V \frac{\partial\lambda_1}{\partial\varepsilon}\frac{2\mu}{\lambda_1}\left\{\lambda_1 Q^{(1)}\left(-2U_{2,2}^{(1)}\right)+2r\left(U_{1,1}^{(1)}U_{2,2}^{(1)}-U_{1,2}^{(1)}U_{2,1}^{(1)}\right)\right\}dV$$

$$=-\frac{4\pi\mu_F h^2}{\lambda_1^F \lambda_1^0}\left\{A_F+\mu_R A_S\right\},\quad A_F=\int_0^{k_F h}F_A(\zeta)d\zeta,\quad A_S=\int_{-\infty}^0 F_A(\zeta)d\zeta,$$

with $F_A = -g'q + r(fg)'$. The expression for b is

$$b=-\frac{(k_F h)^2}{2\lambda_1^F \varepsilon_C}\frac{\left(B_F+\mu_R B_S\right)}{\left(A_F+\mu_R A_S\right)}$$

The four integrals in this expression are evaluated by numerical integration. In these formulas the stretches and wavenumbers are evaluated at $\varepsilon = \varepsilon_C$. As noted earlier, all parameters are determined in terms of r_0^S and μ_R. The coefficient determining the evolution of the mode shape is given by $\hat{u}_2^{(2)} = k_F h G(k_F h)/2\lambda_1^F$.

r	C_{111}	C_{122}	C_{112}	C_{211}	C_{222}	C_{212}
0.2	0.1469	-2.266	0.1406	-0.2407	1.797	-0.4220
0.4	0.2334	-1.167	0.0583	-0.5283	0.4291	-0.5749
0.6	0.3240	-0.7934	0.0318	-0.7045	0.1592	-0.5396
0.8	0.4125	-0.6093	0.0138	-0.8580	0.0524	-0.5156
1	0.5000	-0.5000	0	-1.000	0	-0.5000
1.2	0.5876	-0.4270	-0.0114	-1.134	-0.0285	-0.4896
1.4	0.6755	-0.3746	-0.0210	-1.263	-0.0450	-0.4825
1.6	0.7640	-0.3350	-0.0292	-1.388	-0.0548	-0.4775
1.8	0.8531	-0.3038	-0.0365	-1.509	-0.0608	-0.4740
2	0.9429	-0.2786	-0.0429	-1.629	-0.0643	-0.4714
2.2	1.033	-0.2576	-0.0486	-1.746	-0.0663	-0.4696
2.4	1.124	-0.2400	-0.0538	-1.861	-0.0672	-0.4684
2.6	1.216	-0.2248	-0.0584	-1.975	-0.0674	-0.4675
2.8	1.308	-0.2116	-0.0627	-2.088	-0.0672	-0.4670
3.0	1.400	-0.2000	-0.0667	-2.200	-0.0667	-0.4667

Table 1 $C_{\alpha\beta\gamma}(r)$
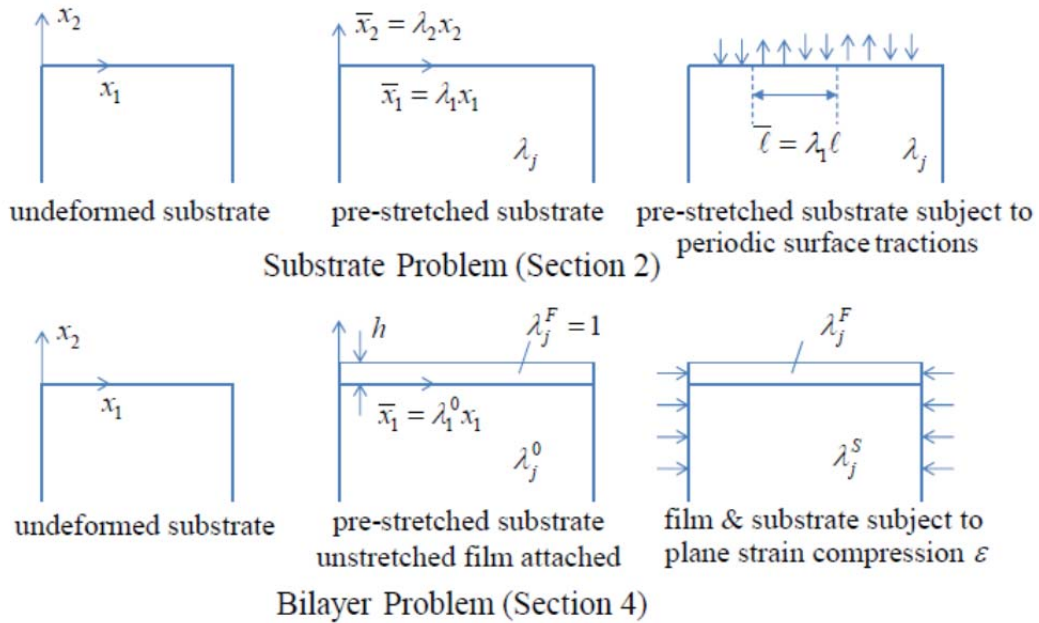
Fig. 1 Geometry and conventions for the problems in Sections 2 and 4.
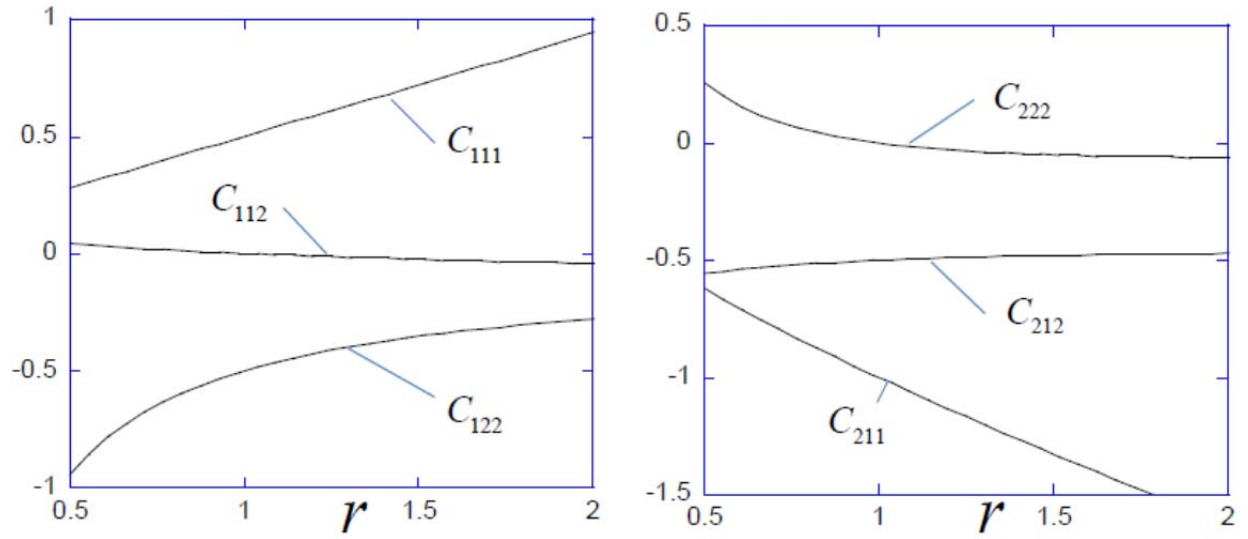
Fig. 2 Dimensionless coefficients in (9) and (14) characterizing the lowest order nonlinear traction-displacement relation of a semi-infinite, incompressible neo-Hookean substrate that has been subject to an initial pre-stretch $(\lambda_1, \lambda_2, \lambda_3)$. The coefficients depend only on $r = \lambda_2 / \lambda_1 = 1 / \lambda_1^2 \lambda_3$ and are listed in Table 1.
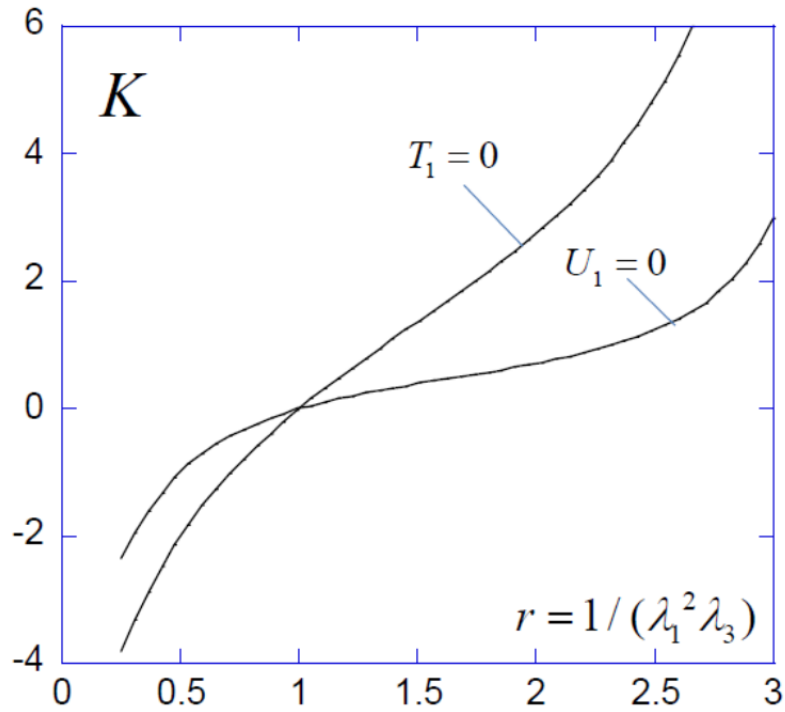
Fig. 3 The coefficient in Eq. (17) governing the lowest order nonlinear traction response of a pre-stretched substrate to an imposed normal sinusoidal surface traction. One curve applies to a substrate whose surface has tangential displacement constraint ($U_1 = 0$) while the other curve applies for no tangential constraint ($T_1 = 0$). The plot holds for any combination of uniform pre-stretch specified by r.
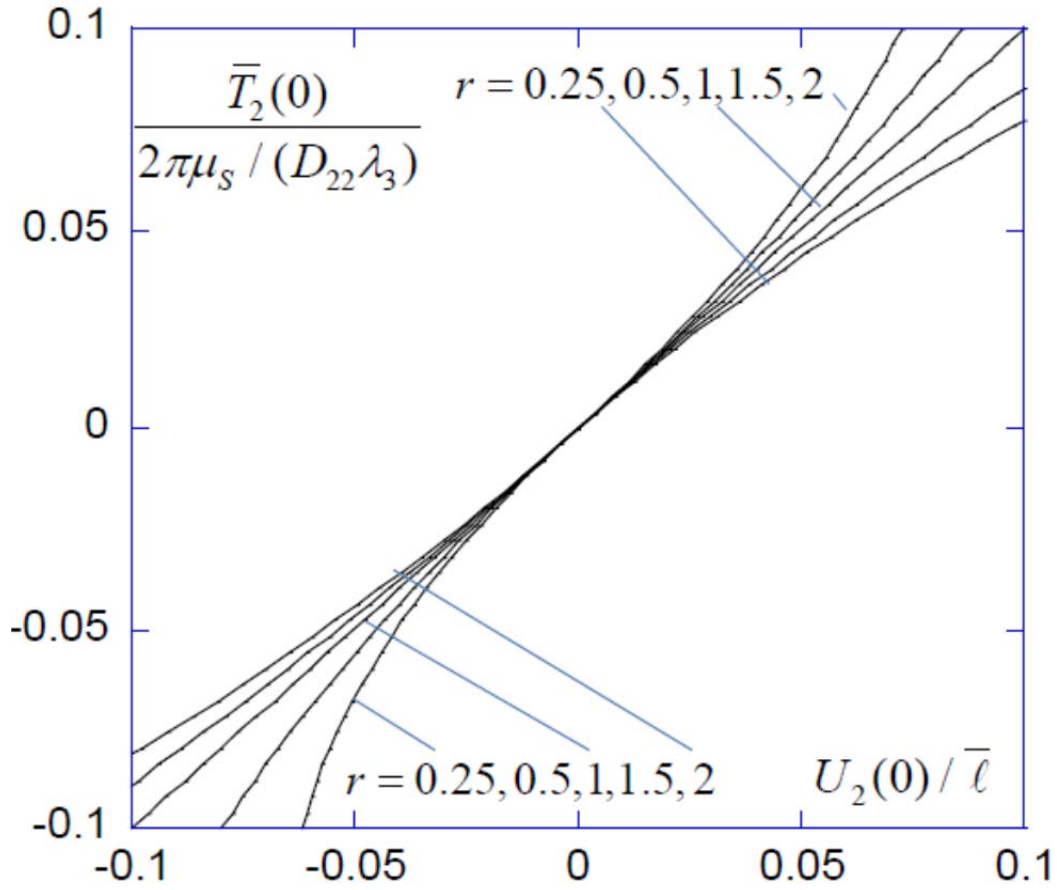
Fig. 4 The effect of pre-stretch as measured by $r = \lambda_2 / \lambda_1 = 1/ \lambda_1^2 \lambda_3$ on the normalized nonlinear traction-displacement behavior in (17) for a neo-Hookean substrate subject to an imposed normal sinusoidal surface traction $\overline{T}_2(x_1) = \overline{T}_2(0)\cos(2\pi \overline{x}_1 / \overline{\ell})$ with $\overline{T}_1 = 0$. Here, $\overline{\ell} = \lambda_1 \ell$ is the wavelength of the imposed traction in the pre-stretched state. If $r < 1$, a softening response occurs for upward deflections and a stiffening response occurs for deflections into the substrate. Conversely, $r > 1$ produces stiffening for upward deflections and softening for downward deflections. To the order computed, this relation is linear if there is no pre-stretch ($r = 1$).
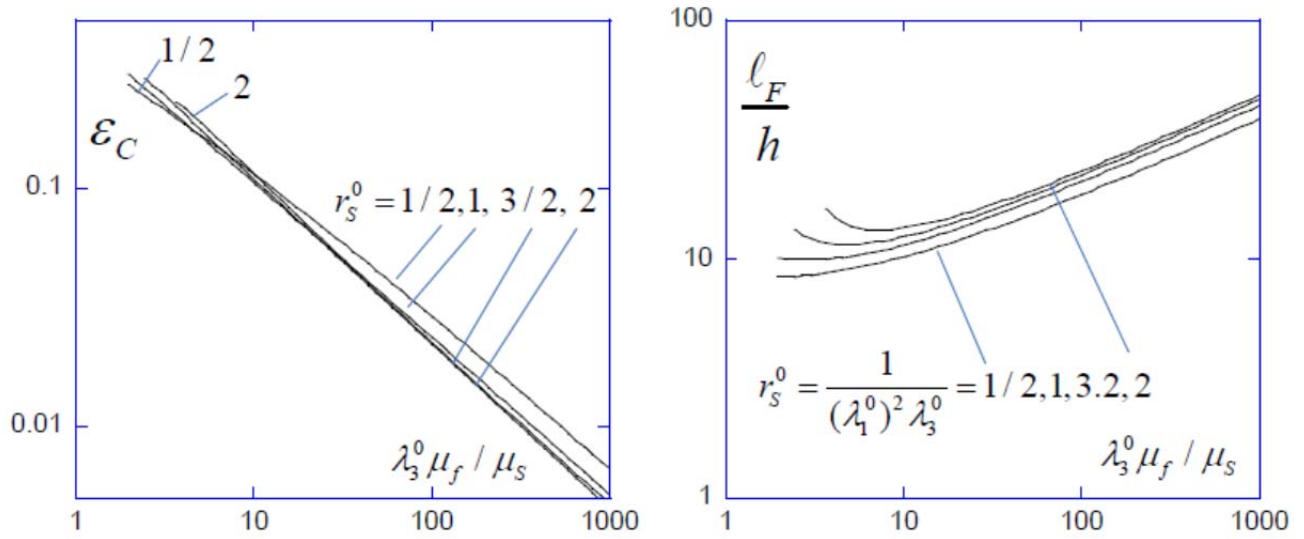
Fig. 5 The compressive nominal strain at bifurcation and the normalized mode wavelength as a function of $1/\mu_R$ for several combinations of substrate pre-stretch as measured by r_S^0.
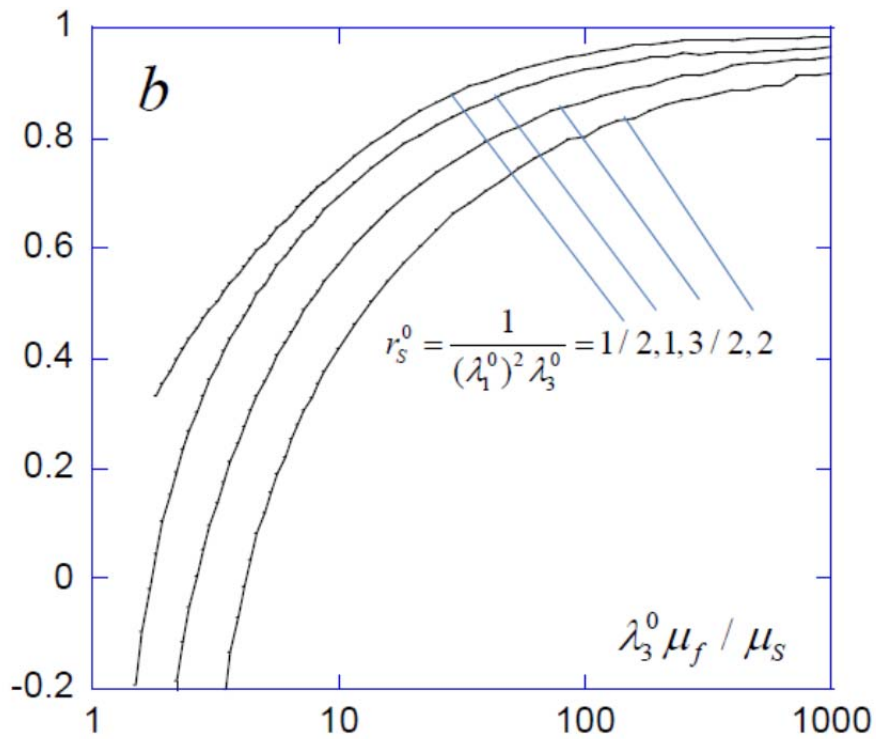

Fig. 6 The initial post-bifurcation coefficient b determining the stability of the bifurcation results in Fig. 5.
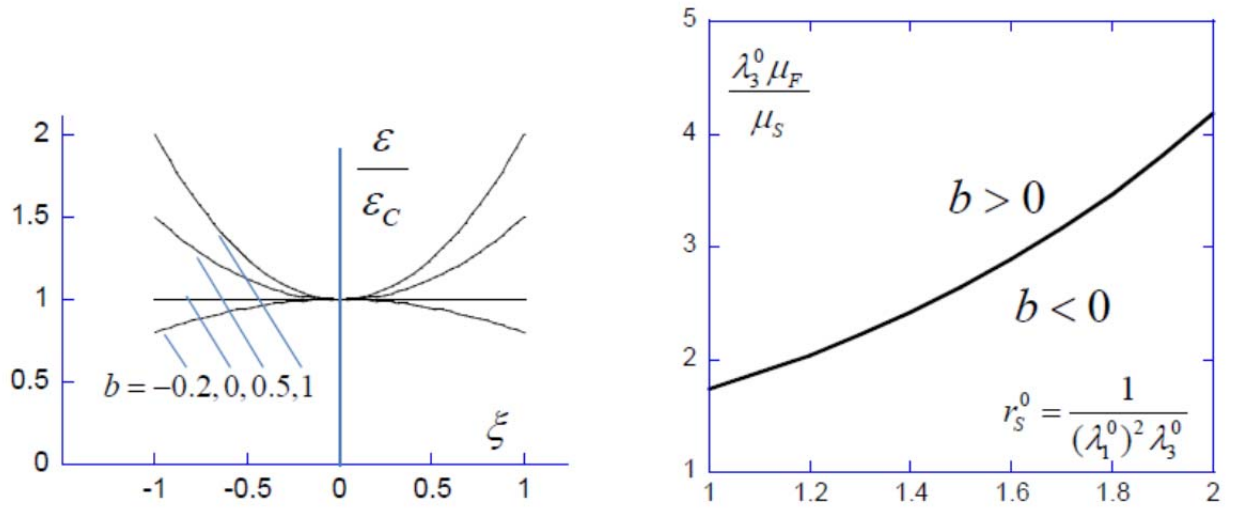
Fig. 7 The relation between the mode amplitude and the compressive strain in the initial post-bifurcation regime (on the left). The boundary between stable bifurcation ($b > 0$) and unstable bifurcation ($b < 0$) in the space of the two parameters characterizing the bilayer (on the right).
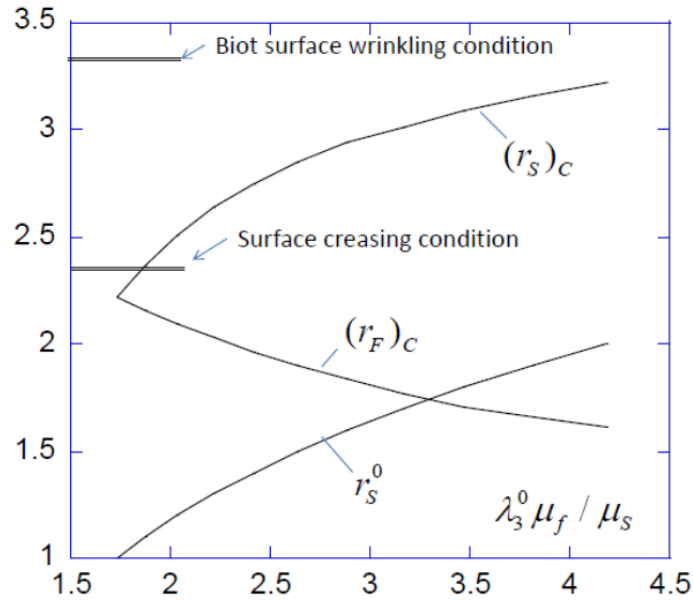

Fig. 8 Values of r_S^0, $(r_F)_C$ and $(r_S)_C$ along the instability boundary in Fig. 7 as a function of $1/\mu_R = \lambda_3^0 \mu_F / \mu_S$. The strains within the film remain below the conditions for localized surface creasing or short-wavelength Biot wrinkling. The strains within the substrate exceed the surface creasing condition if $r_S^0 > 1$.
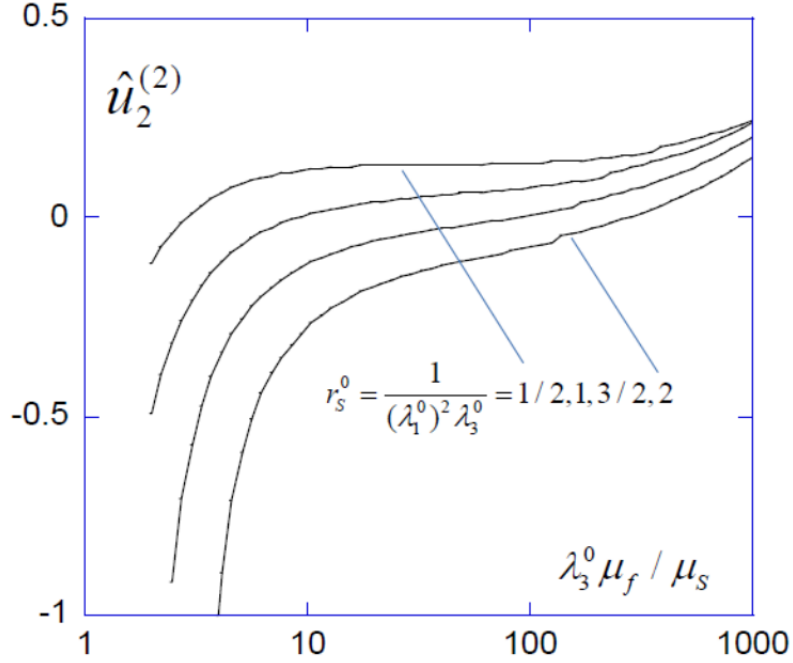
Fig. 9 The dependence of the initial post-bifurcation coefficient $\hat{u}_2^{(2)}$ on substrate pre-stretch, r_S^0, and modulus parameter, $1/\mu_R = \lambda_3^0 \mu_F / \mu_S$.
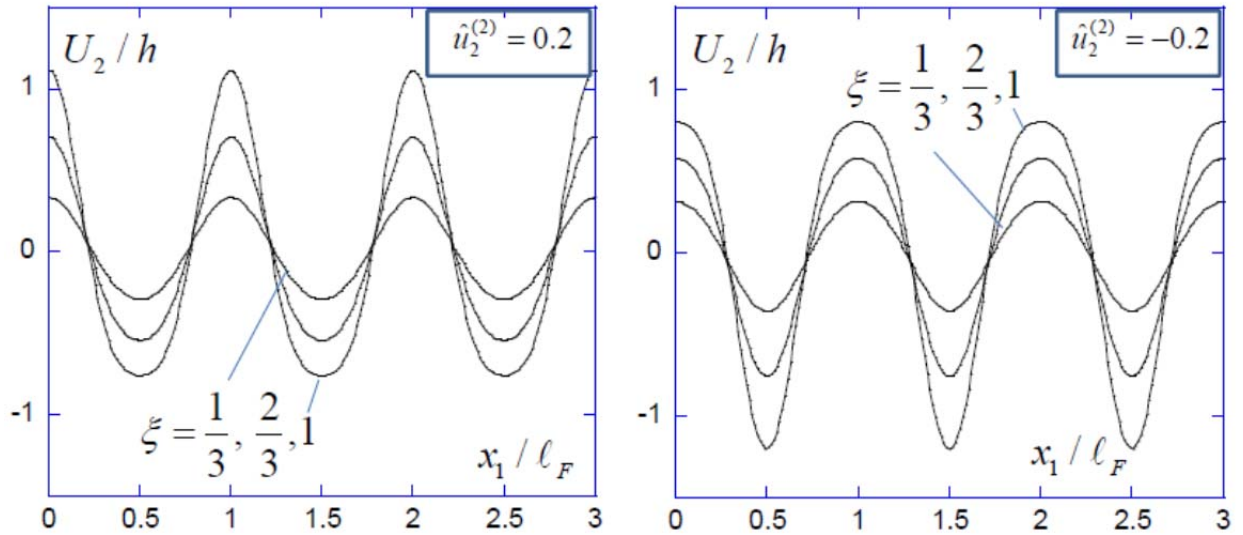

Fig. 10 The evolution of the shape of the normal deflection of the wrinkle mode at the top of the film surface as the mode amplitude, ξ, increases, for $\hat{u}_2^{(2)} = 0.2$ (on the left) and $\hat{u}_2^{(2)} = -0.2$ (on the right). The shape plotted is given by $U_2/h = \xi \cos(2\pi x_1 / \ell_F) + \xi^2 \hat{u}_2^{(2)} \cos(4\pi x_1 / \ell_F)$. The x_1-independent term in (24), $\hat{u}_0^{(2)}$, does not affect the shape.